Sensor-based Globally Asymptotically Stable Range-Only Simultaneous Localization and Mapping

Pedro Lourenço, Pedro Batista, Paulo Oliveira, Carlos Silvestre, and C. L. Philip Chen

Abstract— **Range-only simultaneous localization and mapping is addressed in this paper, through the design, analysis, and experimental validation of a globally asymptotically stable (GAS) filter. A nonlinear sensor-based system is designed and its dynamics augmented so that the proposed formulation can be considered as linear time-varying for the purpose of observability analysis. This allows the establishment of observability results related to the original nonlinear system that naturally lead to the design of a Kalman filter with GAS error dynamics. The performance of the proposed algorithm is assessed resorting to a set of realistic simulations and to the results obtained from experimental tests.**

I. Introduction

Simultaneous Localization and Mapping (SLAM) is the problem of navigating a vehicle in an unknown environment, by building a map of the area and using this map to compute its actual location, without the need for *a priori* knowledge of location. The solution to this problem is of great importance to the field of autonomous robots operating in GPS-denied environments, and therefore SLAM has been subject of intensive research by the community since first proposed in the 1980's. From that initial discussion, a myriad of approaches have arisen. The better known include EKF-SLAM, graph-based solutions, and particle filters (see [1] for a survey of these algorithms). Apart from varying in concept, SLAM approaches also depend on different mapping sensors: SONAR [2], LIDAR [3], monocular and stereo cameras [4] are within the most common. These sensors involve obtaining range and bearing information of the environment, and usually demand the existence of a data association algorithm, due to the unknown correspondence between the reality and the created map. Although localization using distances to beacons is a very well known subject, the number of SLAM algorithms using only ranges is relatively small, especially when compared with the widespread use of algorithms working on range and bearing, or even bearing-only. On one hand, the Range-Only SLAM (RO-SLAM) problem is not prone to association errors, as are the other SLAM formulations, due to the nature of the ranging signals that are usually tagged. On the other hand, one of the main issues in RO-SLAM is the initialization of the algorithm, either due to the absence of global convergence results in EKF solutions, or the computational burden of having a sufficiently representative prior belief, as is the case of approaches resorting to particle filters [5]. Most of the RO-SLAM solutions include some form of initialization procedure before inserting a new landmark in the state, including trilateration with ranges from different instants to obtain a first estimate, usually through least squares, such as what was proposed in [6]. Also, due to the sparse information one may extract from ranging, RO-SLAM algorithms are commonly designed for 2-D environments, e.g., a ground robot and same-height landmarks, see [7]. The common RO-SLAM formulation is closely related to the problem of Sensor Networks (SN), in the sense that there is an agent receiving signals from a network of sensors and, therefore, the two ideas have been used in conjunction in works such as [8], where, along with agent-sensor ranges, sensor-sensor ranges are also used.

This paper introduces a novel RO-SLAM algorithm that eliminates the landmark initialization problem through the establishment of global convergence results with a tridimensional (3-D) sensor-based formulation that avoids the representation of the pose of the vehicle in the state, as is commonly used. Furthermore, the sensor-based approach allows the direct use of odometry-like information that is usually expressed in body-fixed coordinates. This solution is influenced by the source-localization algorithm proposed in [9], as the global convergence results are achieved through a similar state augmentation.

The main contributions of this paper are the design, analysis, and validation of a 3-D RO-SLAM algorithm that i) has Globally Asymptotically Stable (GAS) error dynamics; ii) resorts to the exact linear and angular motion kinematics; iii) uses as odometry-like measurements the linear and angular velocities; iv) solves a nonlinear problem with no linearization whatsoever; and v) builds on the well-established linear time-varying Kalman filter. Note that, although the maps provided by this filter are body-fixed, it is possible to obtain an inertial estimate of both the map and the vehicle pose using, for example, the algorithm proposed in [10]. Aside from simulation, the proposed filter was also validated in real conditions, using Cricket [11] beacons as landmarks and an optical flow procedure to determine the linear velocity.

The paper is organized as follows: in Section II, the problem that is addressed in the paper is stated and the dynamics of the system are presented; the observability analysis of the underlying system is performed in Section III; and filter implementation issues are detailed in Section IV.

This work was partially supported by the FCT [PEst-OE/EEI/LA0009/2011] and by the EU Project TRIDENT (Contract No. 248497). The work of P. Lourenço was supported by the PhD Student Grant SFRH/BD/89337/2012 from the Portuguese FCT POCTI programme.

P. Lourenço, P. Batista, P. Oliveira, and C. Silvestre are with the Institute for Systems and Robotics, Instituto Superior Técnico, Universidade Técnica de Lisboa, Av. Rovisco Pais, 1049-001 Lisboa, Portugal. C. Silvestre and P. Chen are with the Department of Electrical and Computer Engineering, Faculty of Science and Technology of the University of Macau.

{plourenco,pbatista,pjcro,cjs}@isr.ist.utl.pt and philipchen@umac.mo

The results of simulation and real experiments are presented in Sections V and VI, respectively, and, finally, Section VII provides some concluding remarks.

Notation: The superscript ^{I} indicates a vector or matrix expressed in the inertial frame $\{I\}$. For the sake of ease of notation, when no superscript is present, the vector is expressed in the body-fixed frame $\{B\}$. $\mathbf{I}_n$ is the identity matrix of dimension n, and $\mathbf{0}_{n\times m}$ is a n by m matrix filled with zeros. If m is omitted, the matrix is square. $\mathbf{S}[\mathbf{a}]$ is a special skew-symmetric matrix, henceforth called the cross-product matrix, as $\mathbf{S}[\mathbf{a}]\mathbf{b} = \mathbf{a} \times \mathbf{b}$ with $\mathbf{a}, \mathbf{b} \in \mathbb{R}^3$.

II. Problem statement and System dynamics

Consider a vehicle moving in a static world where acoustic beacons are installed at unknown locations, equipped with a sensor suite capable of measuring the linear and angular velocities and receiving radio and acoustic signals from the static beacons, thus being able to compute, through time difference of arrival, the distance to the emitting beacons. This section details a dynamical system that will be used to design a simultaneous localization and mapping filter resorting to the distance between the vehicle and the beacons placed in the environment, and to vehicle motion information.

A. Problem statement

Assume the existence of two frames: a reference inertial frame $\{I\}$ and a body-fixed frame $\{B\}$. Points in the latter frame are mapped to the former through a rotation, given by the rotation matrix $\mathbf{R}(t) \in \mathrm{SO}(3)$ and a translation, given by $^I\mathbf{p}(t) \in \mathbb{R}^3$ that represent, respectively, the orientation and the position of the vehicle. The rotation matrix respects the relation $\dot{\mathbf{R}}(t) = \mathbf{R}(t)\mathbf{S}[\boldsymbol{\omega}(t)]$ where $\boldsymbol{\omega}(t) \in \mathbb{R}^3$ is the angular velocity of the vehicle expressed in the body-fixed frame.

Let $\mathcal{L} := \{1, \ldots, N\}$ be a set of N landmarks present in the environment to be mapped containing, at each instant, N_O observed, or visible, landmarks in the set $\mathcal{L}_O$, and N_U unobserved, or invisible, landmarks in the set $\mathcal{L}_U$ such that $\mathcal{L} = \mathcal{L}_O \cup \mathcal{L}_U$. Furthermore, suppose that $\mathbf{p}_i(t) \in \mathbb{R}^3$ corresponds to a sensor-based landmark in the set $\mathcal{L}$, i.e., the position of the i-th landmark relative to the vehicle, expressed in $\{B\}$, given by $\mathbf{p}_i(t) = \mathbf{R}^T(t)\left(^I\mathbf{p}_i(t) - {}^I\mathbf{p}(t)\right)$. Each landmark is assumed static in the inertial frame, where it is represented by $^I\mathbf{p}_i(t) \in \mathbb{R}^3$. Hence, the dynamics of any landmark expressed in the robotic vehicle coordinate system $\{B\}$ are given by

$$\dot{\mathbf{p}}_i(t) = -\mathbf{S}\left[\boldsymbol{\omega}(t)\right]\mathbf{p}_i(t) - \mathbf{v}(t),$$

where $\mathbf{v}(t) = \mathbf{R}^T(t)\,{}^I\dot{\mathbf{p}}(t) \in \mathbb{R}^3$ is the linear velocity of the vehicle in $\{B\}$. Both the linear and the angular velocities are available through sensor measurements. The distances to landmarks, henceforth denominated ranges, are given by $r_i(t) = \|{}^I\mathbf{p}_i(t) - {}^I\mathbf{p}(t)\| = \|\mathbf{p}_i(t)\|$ and are measured as well. As the landmarks positions are unknown *a priori*, the ranges are not sufficient to obtain estimates of the coordinates of the landmarks, raising the need for the knowledge of the motion of the vehicle. That is why the linear velocity is required to be measured.

This information motivates the design of a system whose states are the sensor-based landmarks and the linear velocity, and with outputs that are the ranges to landmarks and the linear velocity. This system can be expressed through

$$\begin{cases} \dot{\mathbf{p}}_i(t) = -\mathbf{S}\left[\boldsymbol{\omega}(t)\right]\mathbf{p}_i(t) - \mathbf{v}(t) \\ \dot{\mathbf{v}}(t) = \mathbf{0} \\ r_i(t) = \|\mathbf{p}_i(t)\| \\ \mathbf{y}_v(t) = \mathbf{v}(t) \end{cases} \tag{1}$$

with $i \in \mathcal{L}$. The vehicle velocity is assumed, nominally, as constant in the body-fixed frame. Proper tuning of the Kalman filter, considering state disturbances, allows to track slowly time-varying linear velocities.

The problem addressed in this paper is that of designing a navigation system for a vehicle operating in the environment previously described, by means of a filter for the dynamics (1), in the presence of noisy measurements. The algorithm consists of a RO-SLAM filter in the space of sensors, and, therefore, the pose of the vehicle is deterministic as it simply corresponds to the position and attitude of the body-fixed frame expressed in the same frame.

B. Augmented system dynamics

The system derived in the previous subsection is clearly nonlinear, as there is a nonlinear relationship between the output and the system state. The strategy proposed to avoid this nonlinearity is to augment the system state in order to obtain a linear relation between the system state and output, as has been successfully done in [9]. The resulting augmented state is

$$\mathbf{x}(t) := \begin{bmatrix}\mathbf{x}_L^T(t) & \mathbf{x}_V^T(t) & \mathbf{x}_R^T(t)\end{bmatrix}^T,$$

where $\mathbf{x}_L(t) \in \mathbb{R}^{n_L}$ is the stacking of all the landmarks present in the landmark set $\mathcal{L}$, both the visible ones, $\mathbf{x}_{L_O}(t) := \{\mathbf{x}_{L_i}(t),\ i \in \mathcal{L}_O\}$, and the invisible ones, $\mathbf{x}_{L_U}(t) := \{\mathbf{x}_{L_i}(t),\ i \in \mathcal{L}_U\}$, $\mathbf{x}_V(t) \in \mathbb{R}^{n_V}$ represents the vehicle state, i.e., the linear velocity of the vehicle in the body-fixed frame, and $\mathbf{x}_R(t) := \begin{bmatrix}\mathbf{x}_{R_O}^T(t) & \mathbf{x}_{R_U}^T(t)\end{bmatrix}^T \in \mathbb{R}^{n_R}$ contains the ranges to all the landmarks in the visible and invisible sets. In short, the state was defined through

$$\begin{cases} \mathbf{x}_{L_i}(t) := \mathbf{p}_i(t) \\ \mathbf{x}_V(t) := \mathbf{v}(t) \\ x_{R_i}(t) := r_i(t) \end{cases}, \tag{2}$$

where $\mathbf{x}_{L_i}(t) \in \mathbb{R}^3$ and $x_{R_i}(t) \in \mathbb{R}$ are part of the full landmark and full range states, respectively, for all $i \in \mathcal{L}$. It is important to notice that, both in the landmark and range states, the first N_O quantities are the visible ones, while the $i \in \{N_O + 1, \ldots, N_U\}$ are the remaining. The state is chosen in this way to simplify, without loss of generality, the forthcoming analysis.

The dynamics of the landmark and vehicle states have already been defined in (1), hence to obtain the full system dynamics the derivative of the range, given by

$$\dot{r}_i(t) = \frac{1}{r_i(t)}\mathbf{v}(t) \cdot \mathbf{p}_i(t),$$

is needed. Note that, although the system output is now linear, the introduction of the ranges as states has created another nonlinearity in the dynamics. On the other hand, the velocity is directly available as a measurement, as is the distance $r_i(t)$ if the corresponding landmark is visible, i.e.,

if $i \in \mathcal{L}_O$. Therefore, it is possible to replace the dependence on the state by one on the system output. Observing that the system output is given by

$$\mathbf{y}(t) = \begin{bmatrix} \mathbf{y}_v^T(t) & y_{R_1}(t) & \cdots & y_{R_{N_O}}(t) \end{bmatrix}^T,$$

where $\mathbf{y}_v(t) := \mathbf{v}(t)$ and $y_{R_i}(t) = r_i(t)$, $i \in \mathcal{L}$, it is possible to derive the dynamics of the augmented system, which are given by

$$\begin{cases} \dot{\mathbf{x}}(t) = \mathbf{A}_F(\mathbf{x}_{R_U}(t), \mathbf{y}(t), t)\mathbf{x}(t) \\ \mathbf{y}(t) = \mathbf{C}_F\mathbf{x}(t) \end{cases}, \tag{3}$$

where

$$\mathbf{A}_F(\mathbf{x}_{R_U}(t), \mathbf{y}(t), t) = \begin{bmatrix} \mathbf{A}_L(t) & \mathbf{A}_{LV} & \mathbf{0}_{n_L \times n_R} \\ \mathbf{0}_{n_V \times n_L} & \mathbf{0}_{n_V} & \mathbf{0}_{n_V \times n_R} \\ \mathbf{A}_{RL}(\mathbf{x}_{R_U}(t), \mathbf{y}(t), t) & \mathbf{0}_{n_R \times n_V} & \mathbf{0}_{n_R} \end{bmatrix},$$

and

$$\mathbf{C}_F = \begin{bmatrix} \mathbf{0}_{3\times n_L} & \mathbf{I}_3 & \mathbf{0}_{3\times N_O} & \mathbf{0}_{3\times N_U} \\ \mathbf{0}_{N_O\times n_L} & \mathbf{0}_{N_O\times 3} & \mathbf{I}_{N_O} & \mathbf{0}_{N_O\times N_U} \end{bmatrix}.$$

The block matrices that compose the dynamics matrix are given by $\mathbf{A}_L(t) := \operatorname{diag}\left(-\mathbf{S}\left[\boldsymbol{\omega}(t)\right], \ldots, -\mathbf{S}\left[\boldsymbol{\omega}(t)\right]\right)$, $\mathbf{A}_{LV} := \begin{bmatrix} -\mathbf{I}_3 & \cdots & -\mathbf{I}_3 \end{bmatrix}^T$ and

$$\mathbf{A}_{RL}(\mathbf{x}_R(t), \mathbf{y}(t), t) := -\operatorname{diag}\left(\frac{\mathbf{y}_v^T(t)}{y_{R_1}(t)}, \ldots, \frac{\mathbf{y}_v^T(t)}{y_{R_{N_O}}(t)}, \frac{\mathbf{y}_v^T(t)}{x_{R_{N_O+1}}(t)}, \cdots, \frac{\mathbf{y}_v^T(t)}{x_{R_N}(t)}\right).$$

It is clear that the system now derived is still nonlinear, due to the dependence of the dynamics on the velocity and on the ranges. However, as both the first N_O ranges and the linear velocity are measured, the dependence of $\mathbf{A}_{RL}(\mathbf{x}_R(t), \mathbf{y}(t), t)$ in the full range state can be substituted by a dependence on the system output. This is done so that the observability analysis can be performed in a linear fashion, as it will be seen in the next section. Notice also that there are several singularities in the dynamics matrix, if one of the ranges becomes null. To prevent that, the following assumption is needed.

Assumption 1: The motion of the vehicle is such that

$$\underset{i\in\mathcal{L}}{\forall} \quad \underset{t\geq t_0}{\forall} \quad \underset{R_M, R_m>0}{\exists} : \quad R_m < r_i(t) < R_M.$$

Even though this assumption is needed for the dynamics matrix to be well-defined, it is only a very mild assumption, as the vehicle is never coincident, in practice, with a landmark, nor can it be arbitrarily distant.

One final aspect important to retain is the fact that there is nothing in the system dynamics imposing the state relations expressed by (2). Although they could be established through augmented nonlinear outputs, that would invalidate the option to expand the system state in order to obtain a linear time-varying system. Furthermore, the next section presents a result that shows that, under certain conditions, the dynamics of the system directly imposes these constraints.

III. Observability analysis

This section details the observability analysis of the nonlinear system derived in the previous section, both in its original and augmented forms. Sufficient conditions for the observability of the system, with a physical insight on the motion of the vehicle, are obtained, and global convergence results are established.

Although the introduction of the augmented system (3) has removed the output nonlinearity existent in the original nonlinear system (1), the presence of the ranges to invisible landmarks in the dynamics matrix introduces another kind of nonlinearity. Furthermore, given that the only available information with which to obtain $\mathbf{x}_{L_i}(t)$ and $x_{R_i}(t)$ is the corresponding range, it is obvious that the invisible landmarks and their ranges cannot be observable. For this reason, and following the approach used in [12] and [13], the ranges to invisible landmarks and the landmarks themselves are removed from the system state, resulting in a reduced state whose dynamics matrix does not depend on the state, as before, but solely on the system output. Thus, as the output is known, this new system may be regarded as linear time-varying for observability purposes.

For the sake of simplicity, and without loss of generality, in this section it is assumed that there is only one visible landmark, i.e., $\mathcal{L}_O := \{1\}$. This is possible due to the multi-single-range character of the problem. Furthermore, as described, the invisible landmarks are discarded and left out of the new system state. Let $\mathbf{z}(t) = \begin{bmatrix} \mathbf{z}_{L_1}^T(t) & \mathbf{z}_V^T(t) & z_{R_1}(t) \end{bmatrix}^T$ be the new reduced state, and the corresponding system be

$$\begin{cases} \dot{\mathbf{z}}(t) = \mathbf{A}(t)\mathbf{z}(t) \\ \mathbf{y}(t) = \mathbf{C}\mathbf{z}(t) \end{cases}, \tag{4}$$

where the dynamics matrix is given by

$$\mathbf{A}(t) := \begin{bmatrix} \mathbf{A}_{L_O}(t) & \mathbf{A}_{LV_O} & \mathbf{0}_{n_O\times n_R} \\ \mathbf{0}_{n_V\times n_O} & \mathbf{0}_{n_V} & \mathbf{0}_{n_V\times n_R} \\ \mathbf{A}_{RL_O}(t) & \mathbf{0}_{n_{R_O}\times n_V} & \mathbf{0}_{n_{R_O}} \end{bmatrix},$$

and the output matrix is simply

$$\mathbf{C} = \begin{bmatrix} \mathbf{0}_3 & \mathbf{I}_3 & \mathbf{0}_{3\times 1} \\ 0 & 0 & 1 \end{bmatrix}.$$

Note that the blocks that constitute the dynamics matrix are the ones defined in the previous section, while including only the visible landmark. Also, the dependence on the system output and input can be seen as merely a dependence on time, as the two signals are known. This enables to consider (4) as a linear time-varying system (LTV), as shown in [9, Lemma 1]. This will be used throughout this section.

The following result addresses the observability analysis of the LTV system, but before proceeding with the analysis it is necessary to define ${}^I\mathbf{v}(t) = \mathbf{R}(t)\mathbf{v}(t)$ as the linear velocity of the vehicle in the inertial frame $\{I\}$.

Theorem 1: Consider the LTV system given by (4) and let $\mathcal{T} := [t_0, t_f]$. If there exist three instants $\{t_1, t_2, t_3\} \in \mathcal{T}$ such that the linear velocity of the vehicle expressed in the inertial frame is linearly independent in those instants, i.e., $\det\left(\begin{bmatrix} {}^I\mathbf{v}(t_1) & {}^I\mathbf{v}(t_2) & {}^I\mathbf{v}(t_3) \end{bmatrix}\right) \neq 0$, then the system is observable in the sense that, given the system output $\{\mathbf{y}(t),\, t \in \mathcal{T}\}$, the initial condition $\mathbf{z}(t_0)$ is uniquely defined.

Proof: The proof starts by transforming the LTV system through a Lyapunov transformation, to simplify the analysis. A Lyapunov transformation (see [14, Chapter 1, Section 8] for details), preserves the observability properties of the original system. Consider then the tranformation

$$\mathbf{T}(t) = \operatorname{diag}\left(\mathbf{R}(t), \mathbf{I}_3, 1\right),$$

and the transformed system state given by

$$\boldsymbol{\chi}(t) = \mathbf{T}(t)\mathbf{z}(t). \tag{5}$$

It is straightforward to see that $\mathbf{T}(t)$ has a continuous and bounded time derivative, while having a bounded determinant itself, and therefore it is indeed a Lyapunov transformation. This means that it suffices to prove that the transformed system is observable, an approach employed successfully in the past, in works such as [9].

Before proceeding with the proof it is necessary to derive the new system dynamics, by simply taking the first time derivative of (5) and using the inverse transformation $\mathbf{z}(t) = \mathbf{T}^{-1}(t)\boldsymbol{\chi}(t)$, which results in

$$\begin{cases} \dot{\boldsymbol{\chi}}(t) = \boldsymbol{\mathcal{A}}(t)\boldsymbol{\chi}(t) \\ \mathbf{y}(t) = \mathbf{C}\boldsymbol{\chi}(t) \end{cases}, \tag{6}$$

where

$$\boldsymbol{\mathcal{A}}(t) = \begin{bmatrix} \mathbf{0}_3 & -\mathbf{R}(t) & \mathbf{0}_{3\times 1} \\ \mathbf{0}_3 & \mathbf{0}_3 & \mathbf{0}_{3\times 1} \\ -\frac{\mathbf{y}_v^T(t)}{y_{R_1}(t)}\mathbf{R}^T(t) & \mathbf{0}_{1\times 3} & 0 \end{bmatrix}.$$

The proof follows by computing the transition matrix of the transformed system and subsequently the observability Gramian that will help determine whether the system is observable or not. The computation of the transition matrix can be made either using the Peano-Baker series or, in this case, by simply solving $\boldsymbol{\phi}(t,t_0)\boldsymbol{\chi}(t_0) = \boldsymbol{\chi}(t_0) + \int_{t_0}^{t} \boldsymbol{\mathcal{A}}(\tau)\boldsymbol{\chi}(\tau)d\tau$, which gives

$$\boldsymbol{\phi}(t,t_0) = \begin{bmatrix} \mathbf{I}_3 & -\mathbf{R}^{[1]}(t,t_0) & \mathbf{0}_{3\times 1} \\ \mathbf{0}_3 & \mathbf{I}_3 & \mathbf{0}_{3\times 1} \\ -\mathbf{v}^{[0]}(t,t_0) & \mathbf{v}^{[\star]}(t,t_0) & 1 \end{bmatrix},$$

where the following auxiliary quantities were introduced to simplify this expression,

$$\begin{cases} \mathbf{R}^{[1]}(t,t_0) = \displaystyle\int_{t_0}^{\tau} \mathbf{R}(\tau)d\tau \\ \mathbf{v}^{[0]}(t,t_0) = \displaystyle\int_{t_0}^{t} \frac{\mathbf{y}_v^T(\tau)}{y_{R_1}(\tau)}\mathbf{R}^T(\tau)d\tau \\ \mathbf{v}^{[\star]}(t,t_0) = \displaystyle\int_{t_0}^{t} \frac{\mathbf{y}_v^T(\tau)}{y_{R_1}(\tau)}\mathbf{R}^T(\tau)\mathbf{R}^{[1]}(\tau,t_0)d\tau \end{cases}.$$

Having determined the transition matrix of the system in analysis, it is now possible to compute the observability Gramian, given by

$$\boldsymbol{\mathcal{W}}(t_0,t_f) = \int_{t_0}^{t_f} (\mathbf{C}\boldsymbol{\phi}(\tau,t_0))^T\mathbf{C}\boldsymbol{\phi}(\tau,t_0)d\tau. \tag{7}$$

Consider again [9, Lemma 1]. If the observability Gramian now defined is invertible, then the transformed system is observable in the sense that, given the system output $\{\mathbf{y}(t), t \in \mathcal{T}\}$, the initial condition $\boldsymbol{\chi}(t_0)$ is uniquely defined. The proof follows by contraposition. Suppose that the observability Gramian is not invertible, which means that there exists a unit vector $\mathbf{c} = \begin{bmatrix}\mathbf{c}_1^T & \mathbf{c}_2^T & c_3\end{bmatrix}^T \in \mathbb{R}^{n_\chi}$ such that

$$\mathbf{c}^T\boldsymbol{\mathcal{W}}(t_0,t_f)\mathbf{c} = 0. \tag{8}$$

The substitution of (7) in (8) yields

$$\mathbf{c}^T\boldsymbol{\mathcal{W}}(t_0,t_f)\mathbf{c} = \int_{t_0}^{t_f} \|\mathbf{C}\boldsymbol{\phi}(\tau,t_0)\mathbf{c}\|^2 d\tau,$$

where it is possible to replace the argument of the norm in the integral by a vector function $\mathbf{f}(\tau,t_0)$ such that $\mathbf{f}(\tau,t_0) = \operatorname{diag}\left(\mathbf{R}^T(\tau),1\right)\mathbf{C}\boldsymbol{\phi}(\tau,t_0)\mathbf{c}$. Note that $\|\mathbf{f}(\tau,t_0)\| = \|\mathbf{C}\boldsymbol{\phi}(\tau,t_0)\mathbf{c}\|$,

In order for (8) to be true, both $\mathbf{f}(\tau,t_0)$ and $\frac{d}{d\tau}\mathbf{f}(\tau,t_0)$ must be zero for all $\tau \in \mathcal{T}$. Consider now the expressions for $\mathbf{f}(\tau,t_0)$ and its time derivative, given by

$$\mathbf{f}(\tau,t_0) = \begin{bmatrix}\mathbf{c}_2 & f_r(\tau,t_0)\end{bmatrix}^T \tag{9}$$

and

$$\frac{d}{d\tau}\mathbf{f}(\tau,t_0) = \begin{bmatrix}\mathbf{0}_{1\times 3} & \frac{d}{d\tau}f_r(\tau,t_0)\end{bmatrix}^T, \tag{10}$$

respectively. The component associated with the range output is given by

$$f_r(\tau,t_0) = -\mathbf{v}^{[0]}(\tau,t_0)\mathbf{c}_1 + \mathbf{v}^{[\star]}(\tau,t_0)\mathbf{c}_2 + c_3,$$

while its derivative is

$$\frac{d}{d\tau}f_r(\tau,t_0) = -\frac{\mathbf{y}_v^T(\tau)\mathbf{R}^T(\tau)}{y_{R_1}(\tau)}\mathbf{c}_1 + \frac{\mathbf{y}_v^T(\tau)\mathbf{R}^T(\tau)}{y_{R_1}(\tau)}\mathbf{R}^{[1]}(\tau,t_0)\mathbf{c}_2$$

Evaluating (9) at $\tau = t_0$ while equating the result to zero, immediately yields $\mathbf{c}_2 = \mathbf{0}$ and $c_3 = 0$. Making $\frac{d}{d\tau}\mathbf{f}(\tau,t_0) = \mathbf{0}$, given that Assumption 1 is true, leads to the final condition, expressed through

$${}^I\mathbf{v}(\tau)\cdot\mathbf{c}_1 = 0,\ \forall\tau\in\mathcal{T},$$

where ${}^I\mathbf{v}(\tau) = \mathbf{R}(\tau)\mathbf{v}(\tau)$ represents the linear velocity of the vehicle expressed in the inertial frame. This condition implies that either $\mathbf{c}_1 = \mathbf{0}$, which cannot be as $\mathbf{c}$ was assumed to be a unit vector and it has already been shown that $\mathbf{c}_2 = \mathbf{0}$ and $c_3 = 0$, or the linear velocity of the vehicle in the inertial frame for any t_1, t_2, and t_3 in $\mathcal{T}$ is such that

$$\det\left(\begin{bmatrix}{}^I\mathbf{v}(t_1) & {}^I\mathbf{v}(t_2) & {}^I\mathbf{v}(t_3)\end{bmatrix}\right) \tag{11}$$

is zero. Hence, it has been shown that, if the observability Gramian is not invertible, there do not exist three time instants such that the linear velocity of the vehicle on those three time instants span $\mathbb{R}^3$. By contraposition, if (11) is not zero, the observability Gramian is invertible, and, using [9, Lemma 1], it follows that (6) is observable. Furthermore, the LTV system (4) is also observable, as it is related with the system (6) through a Lyapunov transformation, thus concluding the proof. ■

Remark 1: This theorem establishes conditions for the motion of the vehicle, as it allows to conclude that if there are at least three velocity vectors that span $\mathbb{R}^3$, or, equivalently, if the trajectory of the vehicle is not restricted to a line or a plane, the system is observable. Note that, in a trilateration technique, ranges to four non-coplanar vehicle positions are needed. In this case, the motion of the vehicle provides those positions, as Fig. 1 shows.

The LTV system (4) is a reduction of the augmented nonlinear system (3) in the sense that it does not include the invisible landmarks, and assumes the existence of only a single visible landmark. Due to the independence of the landmarks, whichever their number is, the two systems are completely equivalent in terms of observability, discarding the invisible landmarks. Furthermore, care must be taken before extending the observability results of this section to the original nonlinear system (1). As there is nothing imposing the state relations (2), it is not possible to apply

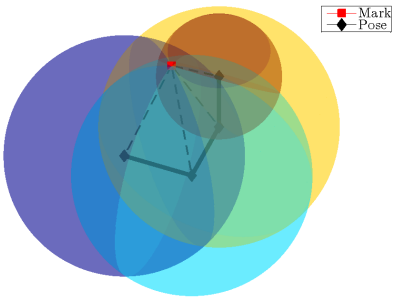

Fig. 1. Trilateration for positioning of a landmark

the results to the original nonlinear system without some reflection. The following result addresses this issue: firstly, the equivalence of the state of the nonlinear and LTV systems is performed in a similar fashion to what was done in [9] and [13]. Secondly, it is shown that the state relations (2) are automatically imposed by the system dynamics when the LTV system is observable.

Theorem 2: Consider the LTV system (4) and the original nonlinear system (1). If the conditions of Theorem 1 hold, then

(i) the state of the original nonlinear system and that of the LTV system are the same and uniquely defined, provided that the invisible landmarks are discarded; and
(ii) a state observer with uniformly globally asymptotically stable error dynamics for the LTV system is also a state observer for the underlying nonlinear system, retaining the same error dynamics properties.

Proof: The proof of the first part of the theorem is made by considering the system output and its relation to the states of the two systems in analysis, leading to a series of equations which, in the conditions of the theorem, result in the correspondence between the states, while imposing the algebraic constraints.

For this purpose, consider the output of the LTV system (4), $\mathbf{y}(t) = \mathbf{C}\mathbf{z}(t)$, and that of the original nonlinear system, $\mathbf{y}(t) = \begin{bmatrix}\mathbf{v}^T(t) & \|r_1(t)\|\end{bmatrix}^T$. Recall that, in this section, it is assumed that the visible landmark set has only one landmark. The comparison of the two outputs shows that

$$\begin{cases}\mathbf{z}_V(t) = \mathbf{v}(t)\\ z_{R_1}(t) = r_1(t)\end{cases}.$$

For the purpose of finding the correspondence of the remaining states, $\mathbf{z}_{L_1}(t)$ and $\mathbf{p}_1(t)$, consider the time evolution of the rotation of each of these states, given by

$$\mathbf{R}(t)\mathbf{z}_{L_1}(t) = \mathbf{R}(t_0)\mathbf{z}_{L_1}(t_0) + \mathbf{R}^{[1]}(t,t_0)\mathbf{z}_V(t_0),$$

and

$$\mathbf{R}(t)\mathbf{p}_1(t) = \mathbf{R}(t_0)\mathbf{p}_1(t_0) + \mathbf{R}^{[1]}(t,t_0)\mathbf{v}(t_0),$$

respectively. This result can be used to compute the derivative of the outputs of the two systems in analysis related to the ranges, which are given by

$$\dot{y}_{R_1}(t) = \frac{\mathbf{y}_v^T(t)\mathbf{R}^T(t)}{y_{R_1}(t)}\left(\mathbf{R}(t_0)\mathbf{z}_{L_1}(t_0) + \mathbf{R}^{[1]}(t,t_0)\mathbf{z}_V(t_0)\right) \tag{12}$$

for the LTV system and

$$\dot{r}_i(t) = \frac{\mathbf{v}^T(t)\mathbf{R}^T(t)}{r_i(t)}\left(\mathbf{R}(t_0)\mathbf{p}_1(t_0) + \mathbf{R}^{[1]}(t,t_0)\mathbf{v}(t_0)\right) \tag{13}$$

for the original nonlinear system. Noting that $\mathbf{z}_V(t) = \mathbf{v}(t)$ and $r_1(t) = y_{R_1}(t)$, and comparing (12) with (13) yields

$$\frac{\mathbf{y}_v^T(t)\mathbf{R}^T(t)}{y_{R_1}(t)}\mathbf{R}(t_0)\left(\mathbf{z}_{L_1}(t_0) - \mathbf{p}_1(t_0)\right) = 0$$

for all t in $\mathcal{T}$. When the conditions of Theorem 1 hold, this expression implies $\mathbf{z}_{L_1}(t_0) = \mathbf{p}_1(t_0)$ by the same reasoning used to prove the sufficiency of these conditions to the observability of the LTV system. Since the dynamics of these states are the same, the equality of the initial conditions implies the equality of the system state. Hence, if the conditions for the observability of the LTV system apply, then the state of the system (4) corresponds directly to that of the original nonlinear system, disregarding the invisible landmarks, thus concluding the proof of the first part of the theorem.

The second part of the theorem follows naturally from the first part. An observer for (4) with globally asymptotically stable error dynamics provides estimates that converge to the true state. Therefore, if the state of the LTV system and that of the original nonlinear system, when the invisible landmarks are discarded, are one and the same, the estimates of the observer will also tend to the true state of system (1) with the same error dynamics. ■

The previous result shows that, if it is possible to design an observer with globally asymptotically stable for the LTV system, this observer will also be suitable for the original nonlinear system. This has established the ground to the design of such a filter, using a linear time-varying Kalman filter, which, to assure the GAS nature of the estimation error dynamics, requires the pair $(\mathbf{A}(t), \mathbf{C})$ to be uniformly completely observable (see [15]). The following theorem addresses this issue.

Theorem 3: Consider system (4) and that Assumption 1 is true. If there exist positive constants $\delta > 0$ and $\alpha^* > 0$ such that, for all $t \geq t_0$, it is possible to choose a set of instants $\{t_1, t_2, t_3\} \in \mathcal{T}_\delta$, with $\mathcal{T}_\delta := [t, t+\delta]$, for which the linear velocity of the vehicle in the inertial frame respects

$$\left|\det\left(\begin{bmatrix}{}^I\mathbf{v}(t_1) & {}^I\mathbf{v}(t_2) & {}^I\mathbf{v}(t_3)\end{bmatrix}\right)\right| > \alpha^*, \tag{14}$$

then the pair $(\mathbf{A}(t), \mathbf{C})$ is uniformly completely observable.

Proof: The concept of uniform complete observability implies uniform bounds on the observability Gramian in time intervals of length δ. It may be expressed through the following statement,

$$\underset{\substack{\delta>0\\ \alpha>0}}{\exists}\quad \underset{t\geq t_0}{\forall}\quad \underset{\substack{\mathbf{c}\in\mathbb{R}^{n_\mathcal{X}}\\ \|\mathbf{c}\|=1}}{\forall}\ :\quad \mathbf{c}^T\boldsymbol{\mathcal{W}}(t,t+\delta)\mathbf{c} \geq \alpha. \tag{15}$$

Hence, the proof consists of studying $\mathbf{c}^T\boldsymbol{\mathcal{W}}(t,t+\delta)\mathbf{c}$ for every possible case of $\mathbf{c} := \begin{bmatrix}\mathbf{c}_1^T & \mathbf{c}_2^T & c_3\end{bmatrix}^T$. However, to simplify the computations, the system in analysis will be the transformed system (6), which is, recalling from (5), related to the LTV system through a Lyapunov transformation, retaining its (uniform complete) observability properties.

Recall the proof of Theorem 1, and the expansion of $\mathbf{c}^T\boldsymbol{\mathcal{W}}(t_0,t_f)\mathbf{c}$ therein, with the definition of $\|\mathbf{f}(\tau,t)\|$ and $\|\frac{d}{d\tau}\mathbf{f}(\tau,t)\|$ in (9) and (10). Then, it is possible to write

$$\|\mathbf{f}(\tau,t)\|^2 = \|\mathbf{c}_2\|^2 + \left(\mathbf{v}^{[0]}(\tau,t)\mathbf{c}_1 - \mathbf{v}^{[\star]}(\tau,t)\mathbf{c_2} - c_3\right)^2.$$

Here, [16, Proposition 4.2] is of great importance in the establishment of the result of this theorem. It states that

if it is possible to find a positive constant β such that $\|\frac{\partial^i}{\partial\tau^i}\mathbf{g}(\tau,t_0)\| > \beta$ then there exists a $\gamma > 0$ such that $\|\mathbf{g}(t_0,t_0+\delta)\| > \gamma$ as long as $\frac{\partial^j}{\partial\tau^j}\mathbf{g}(\tau,t_0)|_{\tau=t_0} = 0$ for all $j < i$ and the norm of the $i+1$-th derivative is upper bounded. It is straightforward to see that this proposition applies to $\mathbf{c}^T\boldsymbol{\mathcal{W}}(t_0,t_f)\mathbf{c}$, and therefore it suffices to show that $\|\mathbf{f}(\tau,t)\|$ is lower bounded for every possible $\mathbf{c}$.

The first condition to study is either $\mathbf{c}_2 \neq \mathbf{0}$, $c_3 \neq 0$ or both, with $\mathbf{c}_1 \in \mathbb{R}^3$. In that case, it is trivial to see that

$$\|\mathbf{f}(t,t)\|^2 \geq \|\mathbf{c}_2\|^2 + c_3^2 := \alpha_1 > 0.$$

The second case involves setting $\mathbf{c}_2$ and c_3 to zero, while leaving $\mathbf{c}_1 \neq \mathbf{0}$. Then, one has $\|\mathbf{f}(t,t)\| = 0$, and [16, Proposition 4.2] applies once more, i.e., if it is shown that there is a τ such that $\left\|\frac{d}{d\tau}\mathbf{f}(\tau,t)\right\|^2 > \alpha_2$, then (15) is true. The computation of this norm is simple, and yields

$$\left\|\frac{d}{d\tau}\mathbf{f}(\tau,t)\right\|^2 = \left(\frac{\mathbf{y}_v^T(\tau)\mathbf{R}^T(\tau)}{y_{R_1}(\tau)}\mathbf{c}_1\right)^2.$$

The objective now is to find, for each $\mathbf{c}_1 \neq \mathbf{0}$, with $\mathbf{c}_2 = \mathbf{0}$ and $c_3 = 0$, a time instant $t^* \in \mathcal{T}_\delta$ such that

$$\left\|\frac{d}{d\tau}\mathbf{f}(\tau,t)\right\|_{\tau=t^*} > \alpha_2.$$

Under the conditions of the theorem, it is straightforward to see that this is always possible. This concludes the enumeration of all the possible values for $\mathbf{c}$, and the proof that, for every possibility, (15) is true, thus proving the sufficiency of the conditions of the theorem for the uniform complete observability of the pair $(\boldsymbol{\mathcal{A}}(t),\mathbf{C})$. Being related to the LTV system (4) through a Lyapunov transformation, this result implies that $(\mathbf{A}(t),\mathbf{C}(t))$ is also uniformly completely observable, and thus the proof of the theorem is concluded. ■

Remark 2: The determinant in (14) can be written as ${}^I\mathbf{v}(t_1)\cdot\left({}^I\mathbf{v}(t_2)\times{}^I\mathbf{v}(t_3)\right)$. Hence, this condition can be understood as a persistent excitation condition, i.e., the velocity at t_1 must be sufficiently out of the plane defined by the velocity at t_2 and t_3 for the vector space defined by them not to degenerate in time.

IV. Filter Design and Implementation

This section addresses the design of the sensor-based RO-SLAM filter. The theoretical results of the previous section were established in a deterministic setting, and thus the presence of measurement noise raises the need for a filtering solution. Theorems 2 and 3 show that it is possible to design an observer with globally asymptotically stable error dynamics for the nonlinear system (1). Hence, a Kalman filter follows naturally for the augmented nonlinear system.

Due to the discrete nature of the available sensor suite, the chosen solution is a discrete time Kalman filter, and thus the continuous-time system (3) must be discretized. Let T_s be the synchronized sampling period of the sensor suite and t_0 be the initial time. Then, the discrete time steps can be expressed through $t_k = kT_s + t_0$, with $k \in \mathbb{N}_O$. Any quantity denoted as $(.)_k$ is the same as $(.)(t_k)$. The process employed was the Euler forward discretization, with a small detail regarding the rotation of a landmark from one instant to the following. For the purpose of obtaining the said rotation, assuming $\boldsymbol{\omega}(t_k)$ constant over each sampling interval, it follows that $\mathbf{R}^T(t_{k+1})\mathbf{R}(t_k) = \exp\left(-\mathbf{S}\left[\boldsymbol{\omega}(t_k)\right]T_s\right)$, and thus it is possible to write the discrete system dynamics

$$\begin{cases}\mathbf{x}_{k+1} = \mathbf{F}_k\mathbf{x}_k + \boldsymbol{\xi}_k \\ \mathbf{y}_{k+1} = \mathbf{H}_{k+1}\mathbf{x}_{k+1} + \boldsymbol{\theta}_{k+1}\end{cases}$$

with

$$\mathbf{F}_k = \begin{bmatrix}\mathbf{F}_{L_k} & \mathbf{I}_3 + T_s\mathbf{A}_{LV} & \mathbf{0}_{n_L\times n_R} \\ \mathbf{0}_{n_V\times n_L} & \mathbf{I}_3 & \mathbf{0}_{n_L\times n_R} \\ \mathbf{I}_3 + T_s\mathbf{A}_{RL_k} & \mathbf{0}_{n_R\times n_V} & \mathbf{I}_3\end{bmatrix},$$

$\mathbf{F}_{L_k} = \operatorname{diag}\left(\mathbf{R}_{k+1}^T\mathbf{R}_k,\ldots,\mathbf{R}_{k+1}^T\mathbf{R}_k\right)$, and $\mathbf{H}_k := \mathbf{C}_F(t_k)$. The vectors $\boldsymbol{\xi}_k$ and $\boldsymbol{\theta}_k$ represent the model disturbance and measurement noise vector, that are assumed to be zero-mean discrete white Gaussian noise.

The signals received from the beacon landmarks are tagged, and therefore, the association of measured data with state data is trivial. For this reason, there is no need for a data association algorithm, nor for a loop closure procedure, which means that the algorithm is a standard discrete time Kalman filter, (see [17]), with the detail that, when a landmark is invisible and its range is unavailable, the estimated range is used in the predict step, allowing the propagation in open loop of the invisible landmarks.

V. Simulation Results

In this section, results from a typical run in a simulation setting are presented. The simulated environment consists of 20 landmarks spread randomly throughout a $16\text{m}\times16\text{m}\times3\text{m}$ map. The trajectory of the vehicle was designed in order to satisfy the observability conditions, and it can be seen in Fig. 2. All the measurements are assumed to be perturbed by zero-mean Gaussian white noise, with standard deviations of $\sigma_\omega = 0.05$ rad/s for the angular rates, $\sigma_v = 0.03$ m/s for the linear velocity, and $\sigma_r = 0.03$ m for the ranges. The Kalman filter parameters were chosen

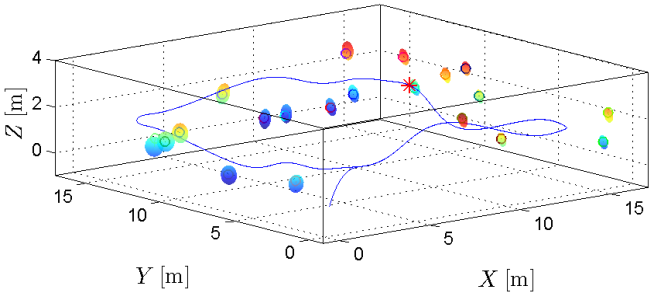

Fig. 2. Picture of the estimated map rotated and translated using the true transformation at $t = 300$ s.

as $\mathbf{Q} = T_s\operatorname{diag}\left(10^{-3}\mathbf{I}_{3N}, 10^{-2}\mathbf{I}_3, 10^{-5}\mathbf{I}_N\right)$ and $\mathbf{R} = 10^{-3}\operatorname{diag}\left(\mathbf{I}_3,\mathbf{I}_{N_O}\right)$. The performance of the RO-SLAM filter can be assessed through Fig. 3, where the norm of the estimation errors of 5 landmarks are presented: it can be seen to converge to a maximum of 10 cm. The estimation error of the velocity is understandably small, as the quantity is directly observed. Its mean is below 10^{-4} m/s and its standard deviation below 10^{-3} m/s. The range error, that grows for invisible landmarks, is 0.0266 m and its standard deviation is 0.0435 m.

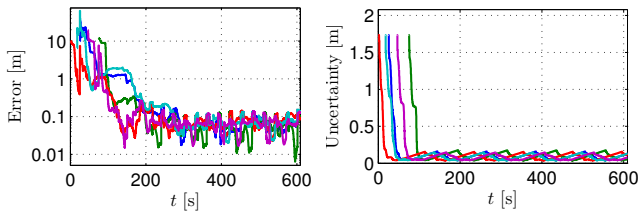

(a) Norm of the error. (b) Uncertainty.

Fig. 3. Evolution of the estimation of 5 landmarks in time.

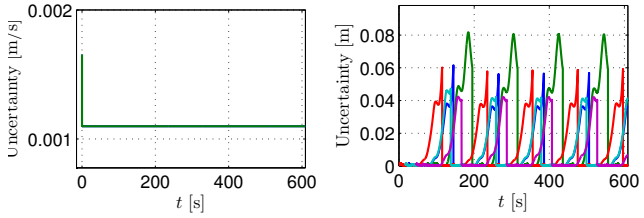

(a) Velocity. (b) Ranges.

Fig. 4. Evolution of the range and velocity estimation standard deviation in time.

The uncertainty associated with each of the estimated quantities is depicted in Fig. 3(b) (the landmark estimates) and Fig. 4 (the ranges and velocity estimates). These results are in accordance with the theoretical results of Section III, as the visible landmarks, as well as the other estimated quantities, converge both in uncertainty and in error.

Finally, an example of the estimated map is given in Fig. 2, where the coloured ellipsoids represent the uncertainty associated ($2\sigma_p$) and the small circles mark the true coordinates of each landmark. Note that the estimated map was rotated and translated to the inertial frame. The red star marks the position of the vehicle at the time of the estimation. Note that the 95% uncertainty ellipsoids surround the true values, as they should.

This simulation was designed to attest the validity of the theoretical results presented in this paper, as well as the convergence properties of the RO-SLAM filter here proposed. It was shown that the algorithm is able to produce a consistent map, depicted in Fig. 2.

VI. Experimental Results

A. Setup

This section details an experiment that took place in the Sensor-based Cooperative Robotics Research Laboratory – SCORE Lab – of the Faculty of Science and Technology of the University of Macau. The experimental setup consists of an *AscTec Pelican* quadrotor instrumented with a *Microstrain 3DM-GX3-25* inertial measurement unit (IMU) working at 200 Hz, a *Microsoft Kinect*, at 10 Hz, a *Crossbow Cricket* receiver, and *VICON* markers. Furthermore, the lab was equipped with 7 more *Crossbow Cricket* motes, emitting sequentially one at a time at 10 Hz (each beacon emits every 700 ms), as well as with a *VICON* Bonita motion capture system, providing accurate estimates of the linear and angular motion quantities of the vehicle, that was used for validation of the estimates provided by the RO-SLAM algorithm.

The cricket beacons emit radio and acoustic pulses that are received by the cricket placed on the vehicle, thus allowing the computation of the ranges through difference between the time of arrival of the two pulses. The facing down camera is used to compute the linear velocity of the vehicle, through the process depicted in Fig. 5. An

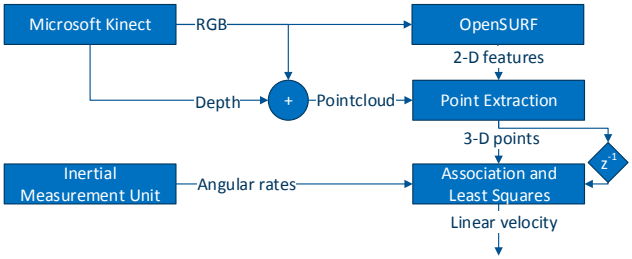

Fig. 5. The process utilized for linear velocity estimation.

implementation of SURF, see [18], detects features in the RGB images that are matched to the pointclouds built using the depth images. The N_k tridimensional features ($\mathbf{f}_k$) of two subsequent frames are associated using a Sequential Compatibility Nearest Neighbour [19] algorithm, and then used in a Least Squares problem to obtain the linear velocity through the following equation

$$\mathbf{v}_k = -\frac{1}{N_k}\begin{bmatrix}\mathbf{I}_3 & \cdots & \mathbf{I}_3\end{bmatrix}\left(\begin{bmatrix}\mathbf{S}\left[\boldsymbol{\omega}_k\right] \\ \vdots \\ \mathbf{S}\left[\boldsymbol{\omega}_k\right]\end{bmatrix} + \frac{\mathbf{f}_{k+1}-\mathbf{f}_k}{T_s}\right),$$

where the angular rates are provided by the IMU. Alternative sensors for the linear velocity of the platform could have been employed.

B. Results

The experiment here detailed consists of series of hand-driven circular-like laps of the quadrotor in a $4\text{m}\times4\text{m}$ area covered by the Cricket constellation. The trajectory, depicted in Fig. 6, was intended to maximize the exposure to each of the beacons, as well as to provide sufficient excitation to the filter.

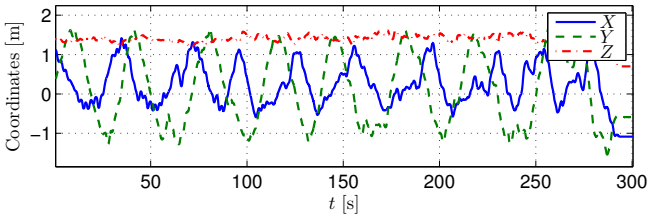

Fig. 6. The position of the vehicle in time.

Figure 7 depicts the estimated position of a landmark against the ground truth data provided by *VICON*. It can be seen that the convergence is very fast in the horizontal plane, represented by Figs. 7(a) and 7(b), and that, after converging, the estimation is very close to ground truth. However, in the vertical axis (Fig. 7(c)), the estimation is much worse, and the convergence is also slower, as it can be seen in Fig. 8

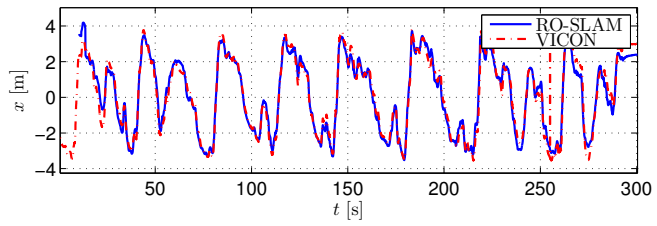

(a) x component

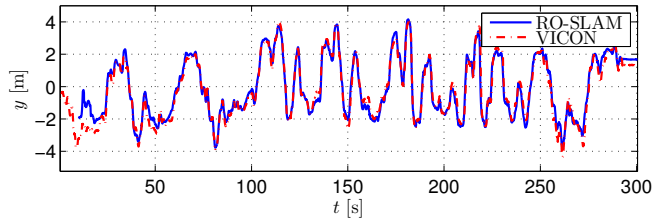

(b) y component

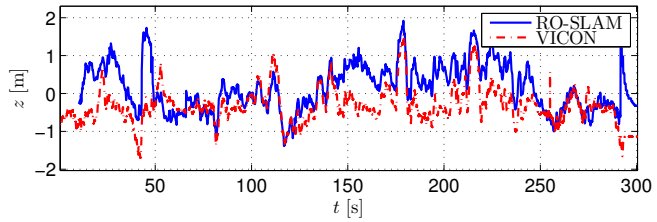

(c) z component

Fig. 7. A sensor-based landmark estimate against ground truth.

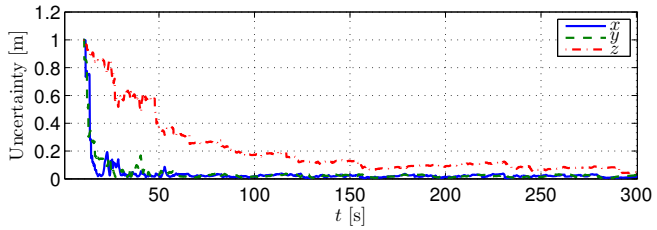

Fig. 8. The estimation standard deviation of the estimates in Fig. 7.

that represents the uncertainty of the estimation. That is due to the less rich trajectory in that axis, as Fig. 6 shows.

These experiments show the good performance of the proposed algorithm in realistic conditions, as well as the need for appropriate trajectories.

VII. Conclusions

This paper presented a novel sensor-based range-only simultaneous localization and mapping filter with globally asymptotically stable error dynamics. This was achieved through state augmentation of a nonlinear system, which, along with the disposal of the non-visible landmarks, enabled regarding the resulting system as linear time-varying. The work focused on the observability analysis of the resulting system, providing theoretical observability guarantees, and equivalence between the systems used in each step of the analysis. These results were followed by the design of a Kalman filter with globally asymptotically stable error dynamics. Simulations allowed for the validation of the theoretical results, and real world experiments illustrated also the good performance of the proposed algorithm. Future work will include the extension of this algorithm to make use of the full capabilities of a sensor network, namely the inter-sensor ranging.

References

[1] H. Durrant-Whyte and T. Bailey, "Simultaneous Localisation and Mapping (SLAM): Part I The Essential Algorithms," *Robotics & Automation Magazine, IEEE*, vol. 13, no. 2, pp. 99–110, 2006.

[2] J. Tardós, J. Neira, P. Newman, and J. Leonard, "Robust mapping and localization in indoor environments using SONAR data," *The International Journal of Robotics Research*, vol. 21, no. 4, p. 311, 2002.

[3] M. Montemerlo, S. Thrun, D. Koller, and B. Wegbreit, "FastSLAM: A Factored Solution to the Simultaneous Localization and Mapping Problem," in *Proceedings of the AAAI National Conference on Artificial Intelligence*. AAAI, 2002, pp. 593–598.

[4] F. Endres, J. Hess, N. Engelhard, J. Sturm, D. Cremers, and W. Burgard, "An Evaluation of the RGB-D SLAM System," in *Proc. of the IEEE Int. Conf. on Robotics and Automation (ICRA)*, St. Paul, MA, USA, May 2012.

[5] J.-L. Blanco, J.-A. Fernandez-Madrigal, and J. Gonzalez, "Efficient probabilistic Range-Only SLAM," in *Proc. 2008 IEEE/RSJ International Conference on Intelligent Robots and Systems, IROS'08*, September 2008, pp. 1017 –1022.

[6] A. Ahmad, S. Huang, J. Wang, and G. Dissanayake, "A new state vector for range-only SLAM," in *Proc. of the 2011 Chinese Control and Decision Conference (CCDC)*, May 2011, pp. 3404 –3409.

[7] E. Menegatti, A. Zanella, S. Zilli, F. Zorzi, and E. Pagello, "Range-only SLAM with a mobile robot and a Wireless Sensor Networks," in *Proc. 2009 IEEE International Conference on Robotics and Automation, ICRA'09*, May 2009, pp. 8 –14.

[8] J. Djugash, S. Singh, G. A. Kantor, and W. Zhang, "Range-Only SLAM for Robots Operating Cooperatively with Sensor Networks," in *Proc. 2006 IEEE International Conference on Robotics and Automation, ICRA'06*, May 2006, pp. 2078 – 2084.

[9] P. Batista, C. Silvestre, and P. Oliveira, "Single range aided navigation and source localization: Observability and filter design," *Systems & Control Letters*, vol. 60, no. 8, pp. 665 – 673, 2011.

[10] P. Lourenço, B. J. Guerreiro, P. Batista, P. Oliveira, and C. Silvestre, "3-D Inertial Trajectory and Map Online Estimation: Building on a GAS Sensor-based SLAM filter," in *European Control Conference 2013*, July 2013, accepted.

[11] N. B. Priyantha, A. Chakraborty, and H. Balakrishnan, "The Cricket Location-Support System," in *Proc. of the Sixth Annual ACM International Conference on Mobile Computing and Networking (MOBICOM)*, August 2000.

[12] B. Guerreiro, P. Batista, C. Silvestre, and P. Oliveira, "Sensor-based Simultaneous Localization and Mapping - Part I: GAS Robocentric Filter," in *Proc. of the 2012 American Control Conference*, Montréal, Canada, Jun. 2012, pp. 6352–6357.

[13] P. Lourenço, B. J. Guerreiro, P. Batista, P. Oliveira, and C. Silvestre, "Preliminary Results on Globally Asymptotically Stable Simultaneous Localization and Mapping in 3-D," in *American Control Conference 2013*, June 2013, accepted.

[14] R. Brockett, *Finite dimensional linear systems*, ser. Series in decision and control. John Wiley & Sons, 1970.

[15] B. Anderson, "Stability properties of Kalman-Bucy filters," *Journal of the Franklin Institute*, vol. 291, no. 2, pp. 137 – 144, 1971.

[16] P. Batista, C. Silvestre, and P. Oliveira, "On the observability of linear motion quantities in navigation systems," *Systems & Control Letters*, vol. 60, no. 2, pp. 101 – 110, 2011.

[17] R. Brown and P. Hwang, *Introduction to random signals and applied Kalman filtering*. Wiley, 1997.

[18] H. Bay, A. Ess, T. Tuytelaars, and L. V. Gool, "Speeded-Up Robust Features (SURF)," *Computer Vision and Image Understanding*, vol. 110, no. 3, pp. 346 – 359, 2008, Similarity Matching in Computer Vision and Multimedia.

[19] J. Neira and J. Tardós, "Data association in stochastic mapping using the joint compatibility test," *Robotics and Automation, IEEE Transactions on*, vol. 17, no. 6, pp. 890 –897, dec 2001.